HHS Public Access

Author manuscript

Dig Dis Sci. Author manuscript; available in PMC 2021 July 01.

Published in final edited form as:

Dig Dis Sci. 2020 July ; 65(7): 2130–2139. doi:10.1007/s10620-019-05915-w.

Morphomic signatures derived from computed tomography predict hepatocellular carcinoma occurrence in cirrhotic patients

Kung-Hao Liang[1,2,10,11,#], **Peng Zhang**[3,4,#], **Chih-Lang Lin**[2,5], **Stewart C. Wang**[3,4], **Tsung-Hui Hu**[6], **Chau-Ting Yeh**[2,7,#], **Grace L. Su**[4,8,9,#]

[1]Department of Medical Research, Taipei Veterans General Hospital, Taipei, Taiwan

[2]Liver Research Center, Chang Gung Memorial Hospital, Linkou, Taiwan

[3]Department of Surgery, University of Michigan Medical School, Ann Arbor, MI, USA

[4]Morphomic Analysis Group, University of Michigan Medical School, Ann Arbor, MI, USA

[5]Liver Research Unit, Keelung Chang Gung Memorial Hospital, Keelung, Taiwan

[6]Division of Hepatogastroenterology, Department of Internal Medicine, Kaohsiung Chang Gung Memorial Hospital, Kaohsiung, Taiwan

[7]Molecular Medicine Research Center, Chang Gung University, Taoyuan, Taiwan

[8]Division of Gastroenterology, University of Michigan Medical School, Ann Arbor, MI, USA

[9]VA Ann Arbor Healthcare System, Ann Arbor, MI, USA

[10]Institute of Food Safety and Health Risk Assessment, National Yang-Ming University, Taipei, Taiwan

[11]Institute of Biomedical Informatics, National Yang-Ming University, Taipei, Taiwan

Abstract

Background & Aims: Computed tomography (CT) provides scans of the human body from which digitized features can be extracted. The aim of this study was to examine the role of these digital biomarkers for predicting subsequent occurrence of hepatocellular carcinoma (HCC) in cirrhotic patients.

Methods: A cohort of 269 patients with cirrhosis were recruited and prospectively followed for the occurrence of HCC in Taiwan. CT scans were retrospectively retrieved and computationally processed using analytic morphomics. A predictive score was constructed using Cox regression and the generalized iterative modeling method, maximizing the log-likelihood of the time to HCC

Corresponding authors: Grace L. Su, MD, VA Ann Arbor Healthcare System, 2215 Fuller Road, Ann Arbor, MI 48105, USA, Tel: 1-7348455865, Fax: 1-7349367392, gsu@umich.edu.
[#]Equal contributions

development. An independent cohort of 274 patients from University of Michigan was utilized to examine the predictive validity of this score in a Western population.

Results: Of the 27 digitized features at the 12th thoracic vertebral level, 6 features were significantly associated with HCC occurrence. Two digitized features (fascia eccentricity and the bone mineral density) was able to stratify patients into high and low-risk groups with distinct cumulative incidence of HCC in both the training and validation cohorts (P = 0.015 and 0.044 respectively). When the two digitized features were tested in the Michigan cohort, only bone mineral density remained an effective predictor.

Conclusion: Digitized features derived from the CT were effective in predicting subsequent occurrence of HCC in cirrhosis patients. The bone mineral density measured on CT was an effective predictor for patients in both Taiwan and USA.

Keywords

bone mineral density; fascia eccentricity; prognosis; retrospective-prospective design

Introduction

Hepatocellular carcinoma (HCC) is an aggressive solid tumor ranking sixth in global incidence of cancers (1). It is also the second leading cause of cancer-related death (1). HCC often occurs in livers with chronic injury, due to persistent hepatitis B and C viral infections (HBV, HCV) or metabolic disorders such as diabetes (2). The risk of HCC increases with progressive liver fibrosis. Once the liver becomes cirrhotic, the risk of HCC is substantial (2%~6% annually) (3), and close surveillance for HCC is recommended (4–6). Although cirrhosis is a known risk factor for development of HCC, the risk is not uniform for all cirrhotic patients. Other known factors include viral load in patients with viral disease such as hepatitis B and C (7–9). In addition to viral factors, there are likely non-viral factors which determine patients' individual risks.

Computed tomography (CT) provides high-resolution scans of the human body in health and disease. CT scans are routinely used for diagnostic purposes where important qualitative information is gathered such as the diagnosis of cirrhosis or hepatocellular carcinoma. While the qualitative readings serve the main purpose for CT scans, immense amounts of quantitative data which is present in these scans are routinely discarded such as liver-specific changes (e.g. liver contour changes and splenomegaly) or measures of muscle mass, bone density, adiposity, and interstitial tissue. Analytic morphomics is a novel computational image processing technology that was developed to extract digitized features such as tissue or organ contours from CT scans (10–28). This technology offers an unprecedented opportunity to extend the use of CT to prognostic purposes. For example, by applying the analytic morphomics technology, we found that the visceral fat density of HCC patients receiving the transcatheter arterial chemoembolization was an effective predictor of subsequent survival, where those with lower visceral fat density survived longer (24).

In this paper, we utilized analytic morphomics to examine the value of digitized features from CT scans of cirrhotic patients, for the purpose of identifying patients at increased risk of the subsequent development of HCC.

Methods

Patients

A cohort of 269 patients were included in this study who had a CT scan prior to the diagnosis of HCC. This study was approved by the institutional review board of the Chang Gung Memorial Hospital, Taiwan (CGMH IRB No. 201600696B0). Patients were recruited from the Keelung (Northern), Linkou (Central-Northern) and Kaohsiung (Southern) branches of the Chang Gung Memorial Hospital, Taiwan. All patients provided written informed consent. The first patient was recruited in January, 2013. The patients were regularly followed until November 18, 2017 or occurrence of HCC. The CT scans and the associated clinical data were then retrospectively retrieved from the hospital database. Patients who were diagnosed with HCC prior to or within the first 4 months (120 days) after the scan was performed were not included in the study. Only one patient died by the end of follow up. A total of 46 HCC events was observed in this cohort. The cumulative incidence of HCC over time after the CT scan is presented as a Kaplan Meier plot in the Supplementary Fig 1A. Patients were assigned to the training cohort or the validation cohort with equal probability using a computational randomization procedure (final assigned number of patients for the two cohorts were 143 and 126 respectively). In the training cohort, the first HCC event occurred at day 126 after CT. Patients were followed for an average of 1130.22 ± 918.01 days (for those with HCC occurrence before the end of follow-up) and 2613.78 ± 821.69 days (for those without HCC) respectively. In the validation cohort, the first HCC event occurred at day 141 after CT. Patients with and without HCC were followed for an average of 801.22 ± 412.62 and 2567.39 ± 760.41 days, respectively.

In HBV patients, life-long antiviral treatment was routinely prescribed if HBV DNA level > 2000 IU/mL. In HCV patients, direct-acting antivirals were not covered by health insurance in Taiwan until 2017. Given that the efficacy of peg-interferon-based antiviral therapy was not satisfactory, and the side effects outweighed its benefit, the majority of patients opted to wait for direct-acting antivirals. Thus, during the period of this study, the HCV patients were in a transitional period waiting for insurance coverage of direct-acting antivirals.

An additional retrospective cohort of cirrhosis patients from University of Michigan Medical School, USA, was used to examine the usefulness of the digitized features in a Western population (N = 274). This retrospective study was approved by the University of Michigan Institutional Review Board. Cirrhosis patients at the University of Michigan Hepatology Clinic who were enrolled in a chronic disease monitoring system (Avitracks, Avicenna Medical Systems, https://www.avicenna-medical.com) (29) from March 1, 2010 to July 30, 2015 and had received an abdominal or chest CT within 365 days of enrollment were included in this study. All patients had a clinical diagnosis of cirrhosis based on imaging, laboratory and/or histological parameters from a board certified gastroenterologist at the University of Michigan and confirmed by the author (G.L.S.) and no diagnosis of HCC on the index CT scan. Patients were followed for an average of 965 days (for those with HCC

occurrence before the end of follow-up) and 1164 days (for those without HCC) respectively. Within this cohort, the average age was 57.7 years old with 55.8% male. 47.1%, 39.8%, and 13.1% were Child-Pugh A, B and C respectively. 28.8% had HCV and 21.5% had Non-alcoholic fatty liver disease. The clinical characteristics of this cohort are provided in Supplementary Table 1.

Analytic morphomics

A series of features, including the body, fat, muscle and spine measures were extracted from the CT images. Digitized features were obtained at the bottom of the twelfth thoracic (T12) vertebral level using the analytic morphomics technology (10–28). A software written in the Matlab computational language was used to capture the features in the CT scans. A complete list of morphomics features is provided in Supplementary Table 2. More information can also be found online at the University of Michigan, the Analytic Morphomics group website: http://www.med.umich.edu/surgerv/morphomics/data_dictionary.html.

Generalized Iterative Modelling for survival analysis

Time-to-event analysis, including Cox regression and the Kaplan Meier plots, were used to analyze the data. Such an analysis not only evaluates the time to HCC occurrence, but also evaluates the time to the end of follow up if HCC has not occurred. Two-tailed P values less than 0.05 were considered statistically significant. Multivariate analysis was also performed by the generalized iterative modelling method for survival analysis (GIM-survival), the predecessor of which was described in (30, 31). The GIM algorithm series has the adaptive learning capability which can identify optimum combinations of variables progressively. It is also compatible to the generalized linear models such as logistic regression or Cox regression. The previous version of GIM maximizes the Mann-Whitney U statistics. In contrast, the current GIM-survival can also maximize the log-likelihood as in the Cox regression, facilitating the time-to-event analysis. The software code of GIM (including GIM-survival) can be freely downloaded at the public-domain Github website (https://github.com/khliang/GIM).

Results

A cohort of 269 liver cirrhotic patients was divided into the training and the validation cohorts by computational randomization procedure (N = 143 and 126 respectively). Between these two cohorts, there was no significant difference in basic demographic factors including age, gender, etiology (HBV, HCV) and Child-Pugh scores (Table 1), as well as their corresponding cumulative incidence (Supplementary Fig.l). We then performed the screening univariate analysis, starting from the time when the CT was taken. In the training cohort, the major viral etiology (HBV and HCV) was not correlated to the HCC occurrence (Table 2). Furthermore, the basic variables of height, weight, body mass index (BMI), alcoholism, Child-Pugh score and platelet count were not significantly associated to the HCC occurrence. The serum Alpha-feto protein levels (AFP) were significantly associated (Table 2). In addition, 6 morphomics variables were significantly associated with the subsequent HCC events, including fascia eccentricity, very low- and normal-density mean

muscle area, dorsal muscle group erector spinae muscle mean intensity, skeletal muscle mean intensity and the trabecular bone mineral density (Table 2). The aim of the current study was to discover surrogate imaging biomarkers that can predict future HCC occurrence, therefore, we used the generalized iterative modeling algorithm to find the optimum combination of these variables for constructing a predictive model, which is:

The hazard function of the patient *i*:

$$H(t|R\_i) = H_0(t)\exp(R\_i)$$

Where the risk score

$$R\_i = -0.02338814 * (\text{fascia eccentricity})^2 * (\text{bone mineral density}) + 3.71863874$$

The score (R_i) was significantly associated with the time-to-HCC in the training cohort (Hazard ratio [HR] = 2.853, 95% Confidence interval [CI] = 1.361 ~ 5.981, P = 0.006). To visualize the relationship between the score and the cumulative incidence of HCC, patients were stratified into tertiles according to the scores (Figure 1A). The cumulative HCC incidence curves of the first and second tertiles are both significantly different from the curve of the third tertile (log-rank P = 0.009 and 0.033 respectively). We then combined the first and second tertiles as the higher risk groups to be compared with the low risk group (i.e. the third tertile); their cumulative incidence differed significantly (P = 0.015, Figure 1B). The score cutoff for separating the two risk groups was 1.605. We then calculated the score of patients in the validation cohort and separated them using the same cutoff. The cumulative incidence of the high- and low-risk groups also differed significantly (P = 0.044, Figure 1C).

We then evaluated the performance of the morphomics HCC score in various subgroups. The association remained statistically significant in both male and female subgroups (P = 0.016 and 0.033 respectively, Figure 2). The association also remained in subjects with the Child-Pugh A (P = 0.009) and with the etiology of chronic hepatitis B (P = 0.001). However, the association was lost in other smaller subgroups such as the hepatitis C patients, or patients with Child-Pugh B or C (Figure 2).

The model incorporated two morphomics variables, the bone mineral density in Hounsfield units (Hu), and the abdominal fascial eccentricity. Figure 3 showed the typical CT images in cirrhosis patients who did not develop HCC during the follow up (Figure 3A and C), and who did subsequently develop HCC during the followup(Figure 3B and D). Eccentricity represents the ratio of the distance between the foci of the ellipse and the major axis length and is a measure of how nearly circular the abdominal facia is. An ellipse whose eccentricity is 0 is actually a circle, while an ellipse whose eccentricity is closest to 1 is a line. (Figure 3 A and B). Cirrhosis patients are less likely to develop HCC if they have higher eccentricity (Figure 3A, eccentricity = 0.78). By contrast, cirrhosis patients with rounder or more circular fascial areas have a higher likelihood of developing HCC (Figure 3B, eccentricity = 0.51). Trabecular bone area density was also measured showing higher bone density in cirrhosis

patients who did not develop HCC (Figure 3 C and D, 253 and 198 Hounsfield units (HU) respectively).

We then investigated the role of age in the occurrence of HCC. The cumulative incidence curves of the first and the second tertiles stratified by their age at CT were both significantly different from that of the third tertile (both $P < 0.001$, Figure 4A). However, there is no significant difference between the first and the second tertiles. Using the GIM-survival software, the age-incorporated morphomics score was generated by combining the age at CT and the morphomics-only score (R_i):

The hazard function of the patient *i*:

$$H(t|S\_i) = H_0(t)exp(S\_i)$$

Where the age-incorporated morphomics score S_*i* is defined as:

$$S\_i = 0.03674825 * age\_i * R\_i + (2.9136) * R\_i - 1.26039598 * R\_i * R\_i$$

Using the age-incorporated morphomics score S_*i*, the cumulative incidence curves of the three tertiles were all significantly different (all pairwise $P \leqq 0.008$, Figure 4B).

To evaluate whether the two major morphomics variables, the bone mineral density and the fascia eccentricity, were independently associated to HCC occurrence, we performed a multivariate analysis. The two variables remained significantly associated to the HCC (adjusted $P = 0.034$ and 0.031 respectively, Supplementary Table 3). A multivariate analysis of AFP and the two variables showed that AFP and bone mineral density remained statistically significant ($P \leqq 0.001$, Supplementary Table 4), while fascia eccentricity was no longer associated to HCC when AFP was incorporated. Using AFP and bone mineral density (BMD) in the training cohort, a new score was generated by the GIM algorithm as:

$$Score = AFP * 0.0127 + BMD * (0.0468) - BMD * BMD * 0.0002$$

This new score was significantly associated with the HCC occurrence in the training cohort (HR = 2.289, 95% CI = 1.417 ~ 3.698, $P = 0.001$, N = 142) and the validation cohort (HR = 1.466, 95% CI = 1.216 ~ 1.768, $P < 0.001$, N = 125). Note one patient in the training cohort and one patient in the validation cohort were not included in the AFP related analysis, because they did not have AFP measurements in their clinical charts.

Application of the digitized features to patients from University of Michigan Hospital

In the University of Michigan Hospital cirrhosis cohort, we tested the scoring systems derived in the Taiwan cohort and found that it was not predictive. We compared the morphomics features and noted significant differences between the two cohorts (Supplementary Table 5). The Michigan cohort was in general larger in size consistent with the higher BMI. One of the most notable difference was the significantly lower fascial eccentricity in the Michigan cohort compared to the Taiwan cohort ($p < 1.0 \times 10^{-57}$)

consistent with more circular shape that is associated with obesity. Recognizing the intrinsic differences in the cohorts, we further examined whether either of the two digital markers (fascial eccentricity and bone mineral density) which comprise the scoring systems had any prediction power. While fascial eccentricity was not predictive of the development of HCC, lower trabecular bone density was predictive with a higher risk of HCC (Figure 5). With regards to AFP, unlike the Taiwan Cohort, the AFP was not predictive of future HCC development in the Michigan cohort.

Discussion

The aim of the current study was to discover surrogate imaging biomarkers that can predict future HCC occurrence. Although CT is not a routine surveillance method for HCC detection in cirrhotic patients, it is often performed to address any abnormalities found on routine surveillance modalities such as ultrasound. In a recent study at the University of Michigan, we found that 25.6% of patients undergoing routine ultrasound surveillance for HCC had abnormality requiring cross-sectional imaging such as CT scan during a median followup of 2.2 years(32). If digital markers were extracted on this clinical CT, it could have the potential to add valuable information to guide future risk and determine if more intensive surveillance was warranted.

Age is a natural factor which cannot be subjected to medical interventions. Therefore, we provided two different HCC risk scores: the morphomics-only risk score (R_i) and the age-incorporated morphomics score (S_i). The former can stratify patients into two risk groups, while the latter can stratify patient into three distinct risk groups. Notably, the morphomic factors were in some degree related to life styles, opening new research directions on the influence of life styles to the risk of HCC.

The low-HCC risk patients tended to have higher bone mineral density and higher fascia eccentricity. We have previously found that higher bone mineral density was associated with improved survival after the liver transplantation for patients with HCC (26). Given the prevalence of vitamin D deficiency and osteoporosis in cirrhosis patients, we hypothesize that bone density may be a surrogate for degree of liver dysfunction and frailty (33). Alternatively, it could be that the decreased bone density may be a surrogate for vitamin D deficiency (common in cirrhosis patients) which has been associated with the development of HCC (34). Given the potential for therapeutic intervention, this would be an important area for future investigation. Fascia eccentricity is a measure that is highly correlated with central obesity as those patients who are more circular carry more abdominal fat while those who are less circular carry less abdominal fat. Abdominal fat including visceral obesity has been associated with increased risk of cancer at multiple sites including esophagus, pancreas, colon, breast, endometrium and kidney (35). Visceral fat is metabolically active and exerts systemic endocrine effects; it is associated with chronic inflammation and changes in insulin and insulin-like growth factor (IGF) that may promote tumorigenesis.

In this study, we found only an association of bone density and not fascial eccentricity with HCC development in the Michigan cohort as compared to the Asian cohort. This is likely due to the distinct differences in the etiology and severity of liver disease. In the Asian

cohort, the majority of patients had viral hepatitis, predominantly hepatitis B as compared to the Michigan cohort where patients were predominantly had NAFLD. We found in our subgroup analysis that our predictive score performed best in the HBV subgroup of patients. In fact, while the predictive score was valid in the HBV subgroup, it was not significantly correlated with HCC occurrence in the HCV and non-B, non-C group. This may account for the difference seen between the Asian and Western cohort as only in the HBV group was the score most effective. Similarly, we have found reports of an association of AFP in the prediction of future HCC in Hepatitis B cohorts(36) which we also found in our Taiwan cohort but this association was not noted in the Michigan cohort. In addition, the majority of patients within the Asian cohort were predominantly Child A patients while those in the Michigan cohort were Child B/C. The prevalence of obesity was much higher in the Michigan population where nearly 2/3 of the population had a BMI of greater than 25. Morphomics feature comparisons between the two groups clearly show significant differences associated with obesity and higher BMI including a very significant difference in baseline fascial eccentricity; this may have obscured the effect of fascial eccentricity in the Michigan cohort.

This study have demonstrated the usefulness of features in CT for the prediction of subsequent HCC occurrence. It is currently unknown whether and how the morphomics features will change after HCC was diagnosed and treated. It is an interesting future direction to evaluate the morphomics features with respect to post-treatment HCC recurrence and patient survival.

In conclusion, digitized features derived from the CT, particularly the bone mineral density and the fascia eccentricity, was effective in predicting subsequent occurrence of HCC in cirrhotic patients in Taiwan. When combined with the age at scan, the predictive score can stratify patients into high, intermediate and low risk groups.

Supplementary Material

Refer to Web version on PubMed Central for supplementary material.

Acknowledgement

The authors would like to thank Brian Derstine, Brian Ross, Dr. Gigin Lin, Dr. Ching-Yi Hsieh, Wan-Ru Liang, Yi-Ting Liao, Yi-Wen Li, Chung-Yin Wu, Fang-Yi He, Hui-Chin Chen, Ya-Ming Cheng, Yu-Jean Chen and Chien-Chih Wang of the liver research center for the excellent technical and administrative assistance.

Ethics and Disclosure:

Neither the submitted material nor portions thereof have been published previously or are under consideration for publication elsewhere. PZ was partially supported by funding from the US National Institutes of Health (KOI DK106296).

SCW and the University of Michigan have a patent on the Morphomics Technique.

SCW has equity interest in Applied Morphomics.

No commercial funding was utilized for this project.

References

1. Ferlay J, Soerjomataram I, Dikshit R, Eser S, Mathers C, Rebelo M, Parkin DM, et al. Cancer incidence and mortality worldwide: Sources, methods and major patterns in GLOBOCAN 2012. International Journal of Cancer 2014;136:E359–E386. [PubMed: 25220842]
2. Huang T-S, Lin C-L, Shyu Y-C, Yeh C-T, Liang K-H, Sun C-C, Lu M-J, et al. Diabetes, hepatocellular carcinoma, and mortality in hepatitis C-infected patients: a population-based cohort study. Journal of Gastroenterology and Hepatology 2016.
3. Fattovich G, Stroffolini T, Zagni I, Donato F. Hepatocellular carcinoma in cirrhosis: Incidence and risk factors. Gastroenterology 2004;127:S35–S50. [PubMed: 15508101]
4. Bruix J, Sherman M. Management of hepatocellular carcinoma. Hepatology 2005;42:1208–1236. [PubMed: 16250051]
5. Liaw Y-F, Kao J-H, Piratvisuth T, Chan HLY, Chien R-N, Liu C-J, Gane E, et al. Asian-Pacific consensus statement on the management of chronic hepatitis B: a 2012 update. Hepatology International 2012;6:531–561. [PubMed: 26201469]
6. Lok ASF. Hepatitis B: Liver fibrosis and hepatocellular carcinoma. Gastroentérologie Clinique et Biologique 2009;33:911–915. [PubMed: 19577871]
7. Yang H-I, Sherman M, Su J, Chen P-J, Liaw Y-F, Iloeje UH, Chen C-J. Nomograms for Risk of Hepatocellular Carcinoma in Patients With Chronic Hepatitis B Virus Infection. Journal of Clinical Oncology 2010;28:2437–2444. [PubMed: 20368541]
8. Lee M-H, Yang H-I, Liu J, Batrla-Utermann R, Jen C-L, Iloeje UH, Lu S-N, et al. Prediction models of long-term Cirrhosis and hepatocellular carcinoma risk in chronic hepatitis B patients: Risk scores integrating host and virus profiles. Hepatology 2013;58:546–554. [PubMed: 23504622]
9. Yang H-I, Yuen M-F, Chan HL-Y, Han K-H, Chen P-J, Kim D-Y, Ahn S-H, et al. Risk estimation for hepatocellular carcinoma in chronic hepatitis B (REACH-B): development and validation of a predictive score. The Lancet Oncology 2011;12:568–574. [PubMed: 21497551]
10. Benjamin AJ, Buschmann MM, Schneider A, Derstine BA, Friedman JF, Wang SC, Dale W, et al. Can Comprehensive Imaging Analysis with Analytic Morphomics and Geriatric Assessment Predict Serious Complications in Patients Undergoing Pancreatic Surgery? Journal of Gastrointestinal Surgery 2017;21:1009–1016. [PubMed: 28342121]
11. Crass RL, Ross BE, Derstine BA, Lichty M, Sullivan JA, Su GL, Wang SC, et al. Measurement of Skeletal Muscle Area Improves Estimation of Aminoglycoside Clearance across Body Size. Antimicrobial Agents and Chemotherapy 2018;62.
12. Cron DC, Noon KA, Cote DR, Terjimanian MN, Augustine JJ, Wang SC, Englesbe MJ, et al. Using analytic morphomics to describe body composition associated with post-kidney transplantation diabetes mellitus. Clinical Transplantation 2017;31:e13040.
13. Derstine BA, Holcombe SA, Goulson RL, Ross BE, Wang NC, Sullivan JA, Su GL, et al. Quantifying Sarcopenia Reference Values Using Lumbar and Thoracic Muscle Areas in a Healthy Population. The journal of nutrition, health & aging 2018;22:180–185.
14. Derstine BA, Holcombe SA, Ross BE, Wang NC, Su GL, Wang SC. Skeletal muscle cutoff values for sarcopenia diagnosis using T10 to L5 measurements in a healthy US population. Scientific Reports 2018;8.
15. Harbaugh C, Henderson B, Zhang P, Derstine B, Holcombe SA, Wang S, Ehrlich PF. The ‘Cushion Effect’ Is Not Protective for Children Involved in Motor Vehicle Crashes. Journal of the American College of Surgeons 2017;225:e187–e188.
16. Harbaugh CM, Zhang P, Henderson B, Derstine BA, Holcombe SA, Wang SC, Kohoyda-Inglis C, et al. Personalized medicine: Enhancing our understanding of pediatric growth with analytic morphomics. Journal of Pediatric Surgery 2017;52:837–842. [PubMed: 28189451]
17. Harbaugh CM, Zhang P, Henderson B, Derstine BA, Holcombe SA, Wang SC, Kohoyda-Inglis C, et al. Evaluating the “cushion effect” among children in frontal motor vehicle crashes. Journal of Pediatric Surgery 2018;53:1033–1036. [PubMed: 29519566]
18. Heckman KM, Otemuyiwa B, Chenevert TL, Malyarenko D, Derstine BA, Wang SC, Davenport MS. Validation of a DIXON-based fat quantification technique for the measurement of visceral fat using a CT-based reference standard. Abdominal Radiology 2018.

19. Holcombe SA, Hwang E, Derstine BA, Wang SC. Measuring rib cortical bone thickness and cross section from CT. Medical Image Analysis 2018;49:27–34. [PubMed: 30031288]
20. Holcombe SA, Wang SC, Grotberg JB. The effect of age and demographics on rib shape. Journal of Anatomy 2017;231:229–247. [PubMed: 28612467]
21. Lee C, Raymond E, Derstine BA, Glazer JM, Goulson R, Rajasekaran A, Cherry-Bukowiec J, et al. Morphomic Malnutrition Score: A Standardized Screening Tool for Severe Malnutrition in Adults. Journal of Parenteral and Enteral Nutrition 2018;42:1263–1271. [PubMed: 29786877]
22. Miller AL, Englesbe MJ, Diehl KM, Chan C- L, Cron DC, Derstine BA, Palazzolo WC, et al. Preoperative Psoas Muscle Size Predicts Postoperative Delirium in Older Adults Undergoing Surgery: A Pilot Cohort Study. Journal of the American Geriatrics Society 2016;65:e23–e24. [PubMed: 27991649]
23. Otemuyiwa B, Derstine BA, Zhang P, Wong SL, Sabel MS, Redman BG, Wang SC, et al. Dorsal Muscle Attenuation May Predict Failure to Respond to Interleukin-2 Therapy in Metastatic Renal Cell Carcinoma. Academic Radiology 2017;24:1094–1100. [PubMed: 28341412]
24. Parikh ND, Zhang P, Singal AG, Derstine BA, Krishnamurthy V, Barman P, Waljee AK, et al. Body Composition Predicts Survival in Patients with Hepatocellular Carcinoma Treated with Transarterial Chemoembolization. Cancer Research and Treatment 2018;50:530–537. [PubMed: 28602057]
25. Pienta MJ, Zhang P, Derstine BA, Enchakalody B, Weir WB, Grenda T, Goulson R, et al. Analytic Morphomics Predict Outcomes After Lung Transplantation. The Annals of Thoracic Surgery 2018;105:399–405. [PubMed: 29198627]
26. Sharma P, Parikh ND, Yu J, Barman P, Derstine BA, Sonnenday CJ, Wang SC, et al. Bone mineral density predicts posttransplant survival among hepatocellular carcinoma liver transplant recipients. Liver Transplantation 2016;22:1092–1098. [PubMed: 27064263]
27. Stidham RW, Waljee AK, Day NM, Bergmans CL, Zahn KM, Higgins PDR, Wang SC, et al. Body Fat Composition Assessment Using Analytic Morphomics Predicts Infectious Complications After Bowel Resection in Crohn's Disease. Inflammatory Bowel Diseases 2015:1.
28. Terjimanian MN, Underwood PW, Cron DC, Augustine JJ, Noon KA, Cote DA, Wang SC, et al. Morphometric age and survival following kidney transplantation. Clinical Transplantation 2017;31:e13066.
29. Aberra FB, Essenmacher M, Fisher N, Volk ML. Quality improvement measures lead to higher surveillance rates for hepatocellular carcinoma in patients with cirrhosis. Dig Dis Sci 2013;58:1157–1160. [PubMed: 23111632]
30. Huang Y-H, Liang K-H, Chien R-N, Hu T-H, Lin K-H, Hsu C-W, Lin C-L, et al. A Circulating MicroRNA Signature Capable of Assessing the Risk of Hepatocellular Carcinoma in Cirrhotic Patients. Scientific Reports 2017;7.
31. Liang K-H, Ahn SH, Lee HW, Huang Y-H, Chien R-N, Hu T-H, Lin K-H, et al. A novel risk score for hepatocellular carcinoma in Asian cirrhotic patients: a multicentre prospective cohort study. Scientific Reports 2018;8.
32. Konerman MA, Verma A, Zhao B, Singal AG, Lok AS, Parikh ND. Frequency and Outcomes of Abnormal Imaging in Patients With Cirrhosis Enrolled in a Hepatocellular Carcinoma Surveillance Program. Liver Transpl 2019;25:369–379. [PubMed: 30582779]
33. Santos LA, Romeiro FG. Diagnosis and Management of Cirrhosis-Related Osteoporosis. Biomed Res Int 2016;2016:1423462. [PubMed: 27840821]
34. Wu DB, Wang ML, Chen EQ, Tang H. New insights into the role of vitamin D in hepatocellular carcinoma. Expert Rev Gastroenterol Hepatol 2018;12:287–294. [PubMed: 29140126]
35. Miles LM. Food, nutrition, physical activity and the prevention of cancer: a global perspective - the WCRF/AICR second report. Nutrition Bulletin 2005;30:168–172.
36. Hann HW, Fu X, Myers RE, Hann RS, Wan S, Kim SH, Au N, et al. Predictive value of alpha-fetoprotein in the long-term risk of developing hepatocellular carcinoma in patients with hepatitis B virus infection--results from a clinic-based longitudinal cohort. Eur J Cancer 2012;48:2319–2327. [PubMed: 22436980]

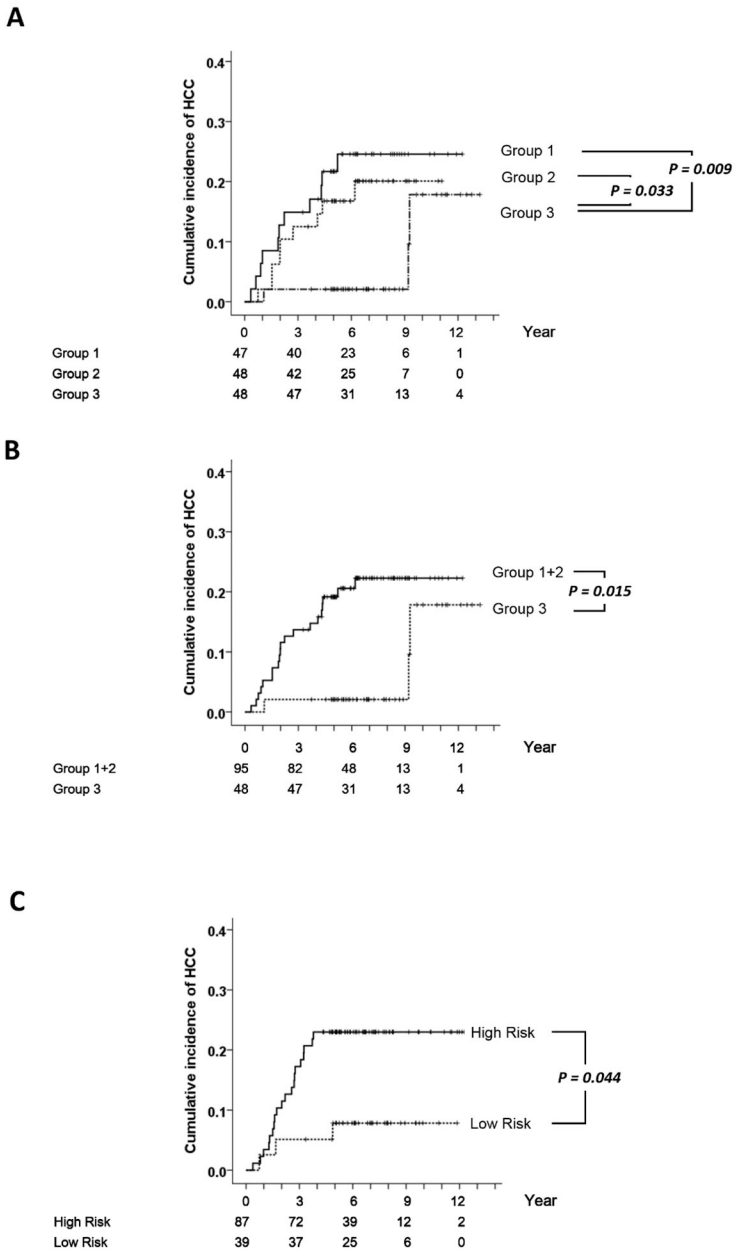

Figure 1.

The cumulative incidence of HCC of patients stratified by the morphomics HCC risk score. The horizontal axes correspond to the time after CT. (A) The training cohort when patients were divided into tertile groups by the score. Group 1: the first tertile (N = 47). Group 2: the second tertile (N = 48). Group 3: the third tertile (N = 48). (B) The training cohort when groups 1 and 2 were merged together. (C) The validation cohort when patients were stratified using the same cutoff as in the training cohort (N = 87 and 39 respectively).

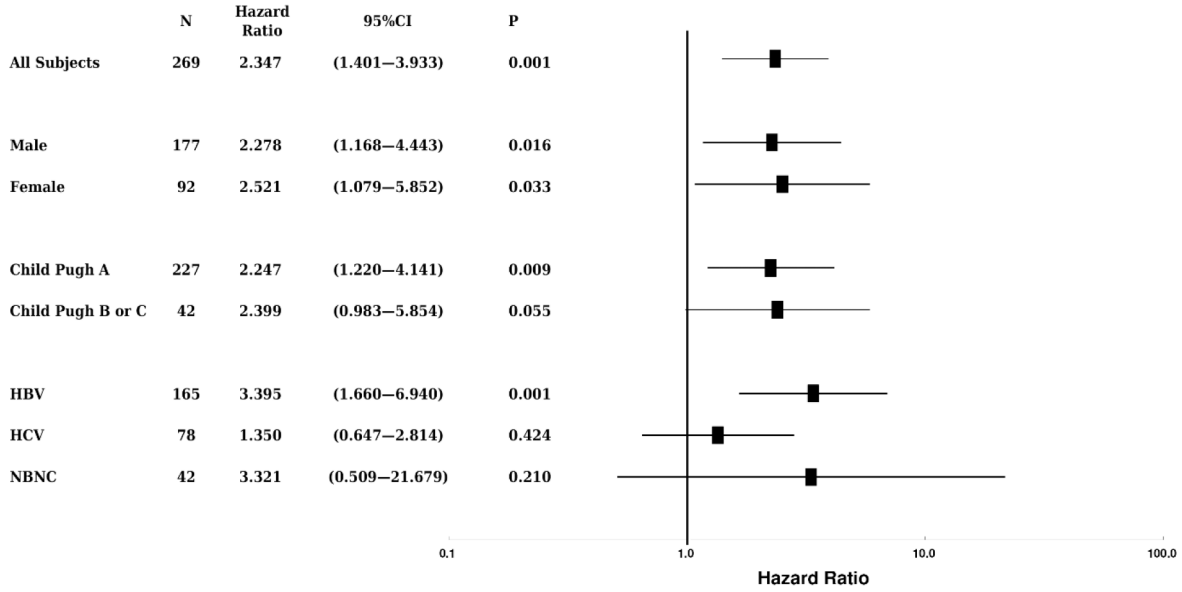

Figure 2.

The distributions of hazard ratios in various patient subgroups. The morphomics HCC scores were associated to subsequent HCC occurrence in male, female, Child Pugh A and HBV subgroups. N: sample size. CI: confidence Interval. NBNC: neither hepatitis B nor C.

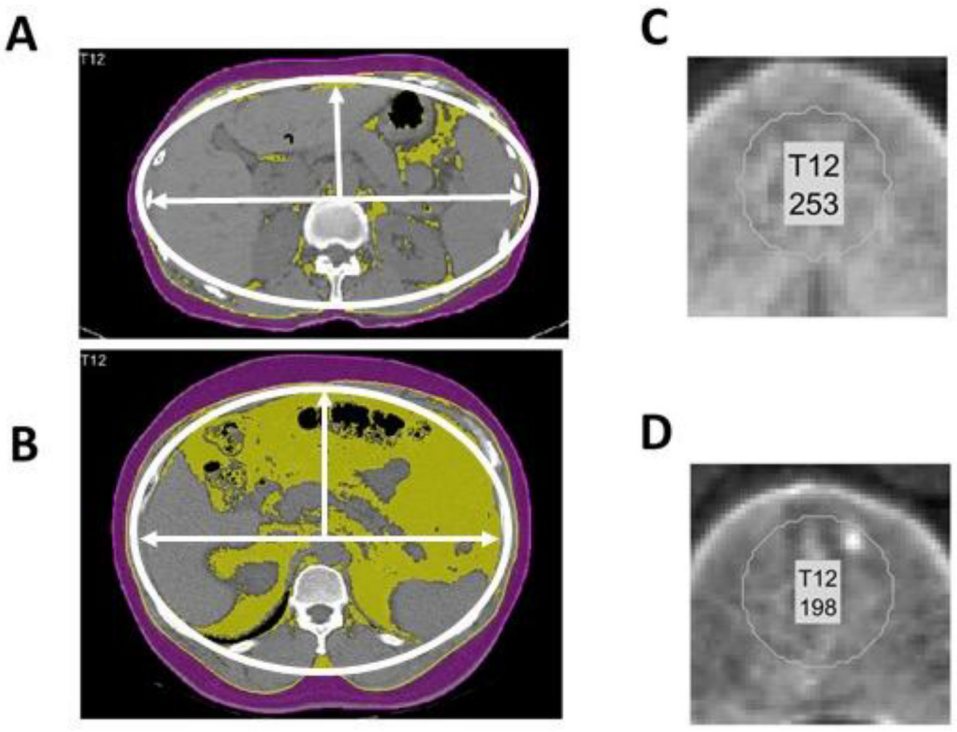

Figure 3.

(A, B) CT scans overlaid with the fascia contour (a thin white curve) which were used to calculate its eccentricity. (C, D) The zooming-in view of the trabecular bone region of the spine which were used for the estimation of bone mineral density in the Hounsfield numbers (Hu). (A, C) Sample patient scan with liver cirrhosis without subsequent HCC by the end of the follow up. (B, D) Sample patient scan taken more than 4 months before the diagnosis of HCC.

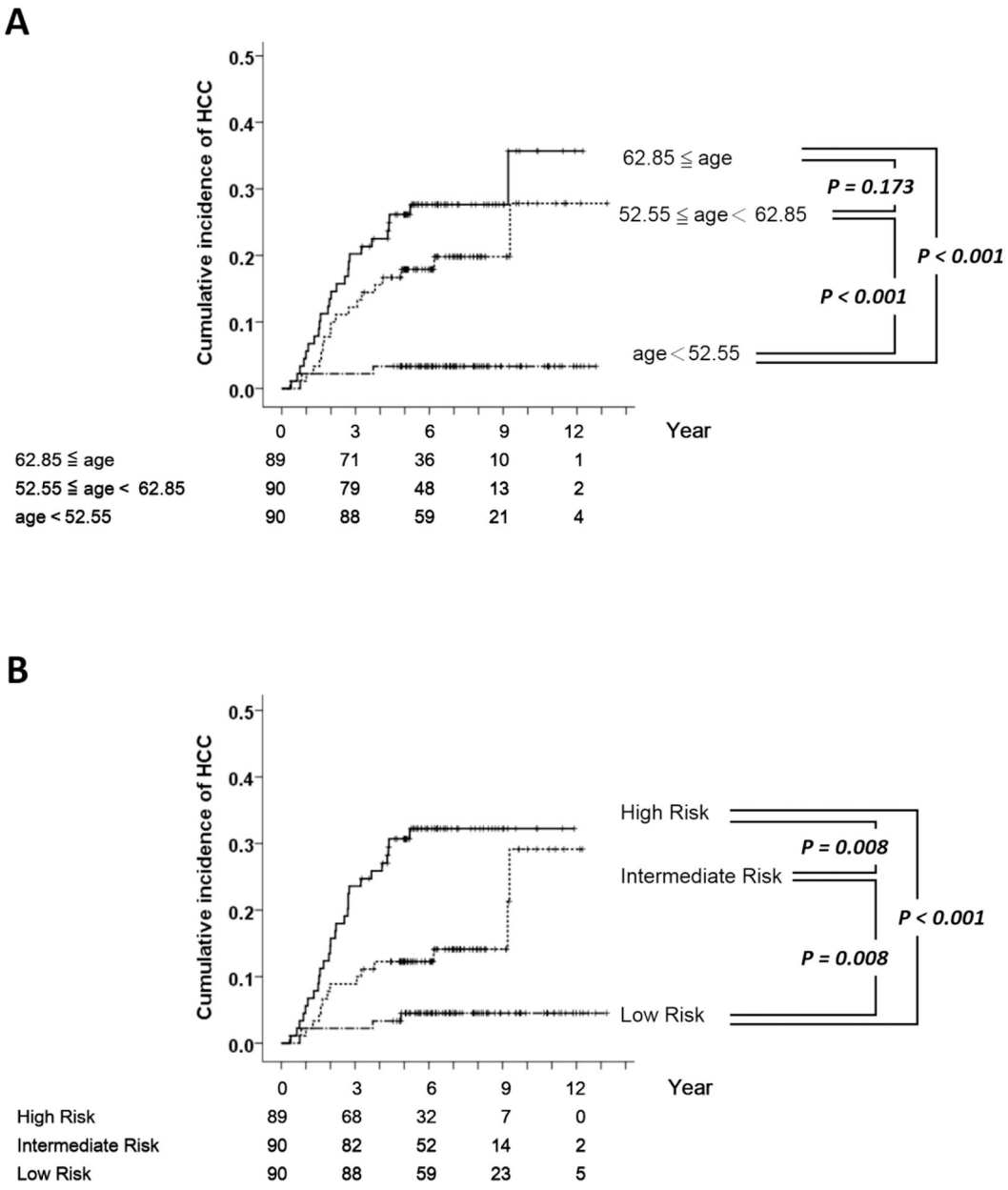

Figure 4.

(A) The cumulative incidence of HCC in patients stratified by age at CT (the first tertile N = 89; the second tertile N = 90; the third tertile N = 90). (B) The cumulative incidence of HCC in patients stratified by the age-incorporated morphomics HCC score (high-risk group N = 89; intermediate risk group N = 90; low risk group N = 90).

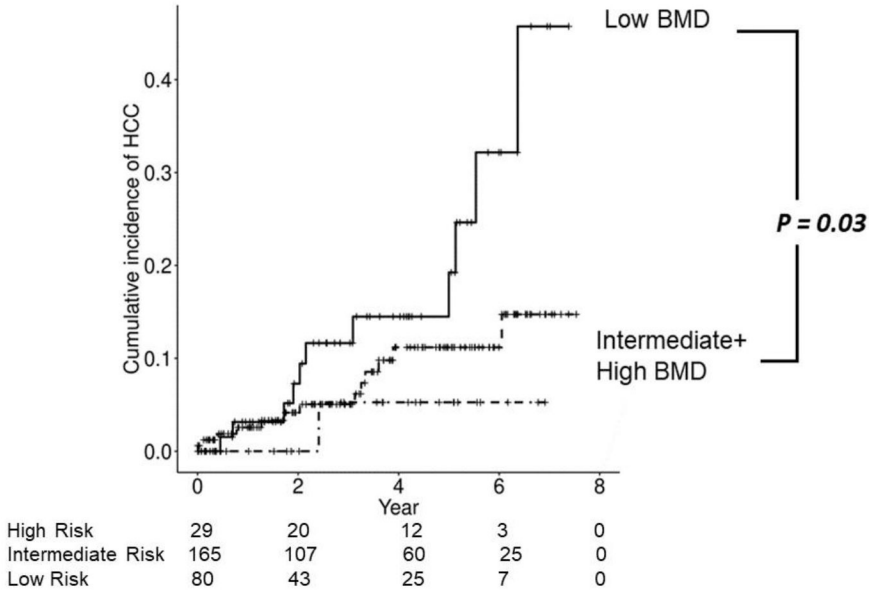

Figure 5.

The cumulative incidence plot of HCC occurrence in patients stratified by the bone mineral density as tertiles. Compared to the middle and highest tertile of bone density, the patients with the lowest bone density had significantly higher risk of HCC (p=0.03, log-rank test)

Table 1.

Clinical characteristics of the training and validation cohorts.

Variable	Training Cohort	Validation Cohort	P
Subject number	143	126	
Gender			0.981
Male (%)	94 (65.73%)	83 (65.87%)	
Female (%)	49 (34.27%)	43(34.13%)	
Child Pugh Score			0.331
A	125 (87.41%)	102 (80.95%)	
B	16(11.19%)	22 (17.46%)	
C	2(1.40%)	2(1.59%)	
Age at CT	57.65 ± 11.31	56.58 ±11.36	0.441
HBV	92 (64.34%)	73 (57.94%)	0.282
HCV	40 (27.97%)	38(30.16%)	0.693
AST (IU/L)	43.15 ±30.14	48.57 ±37.52	0.196
ALT (IU/L)	36.23 ±21.67	43.04 ±44.55	0.120
HDL (mg/dL)	50.59 ±16.35	47.19 ±14.52	0.072
Sugar AC (mg/dL)	104.97 ±28.21	107.09 ±38.71	0.613
Insulin (mIU/L)	10.77 ± 11.25	13.21 ± 13.31	0.109
Sugar/Insulin ratio	21.06 ±63.85	12.76 ±8.91	0.126
HOMA-IR	3.00 ±3.93	3.88 ±5.97	0.161

HOMA-IR: Homeostatic model assessment of insulin resistance

Table 2.

Univariate analysis of the association of variables with the subsequent occurrence of hepatocellular carcinoma.

Variable	Hazard Ratio	95% confidence interval		P
Basic Information				
Gender-Male	0.961	0.407	2.266	0.927
height	0.045	0.000	75.949	0.413
weight	0.973	0.933	1.015	0.202
BMI	0.000	0.000	Inf	0.388
HBV	0.496	0.184	1.335	0.165
HCV	0.715	0.303	1.688	0.444
Alcoholism	0.045	0.000	75.949	0.413
Child Pugh (B+C vs. A)	1.518	0.516	4.464	0.448
platelet	0.992	0.983	1.000	0.052
Serum biochemistry				
AST	1.005	0.995	1.015	0.296
ALT	1.002	0.984	1.021	0.845
AFP	1.015	1.006	1.023	**0.001**
HDL	0.987	0.959	1.014	0.339
Sugar AC	1.000	0.985	1.015	0.999
Insulin	0.994	0.954	1.034	0.750
Sugar/Insulin ratio	0.998	0.983	1.012	0.764
HOMA-IR	0.969	0.850	1.106	0.643
Body Measures				
body depth	1.003	0.986	1.021	0.715
body width	0.991	0.975	1.008	0.297
fascia to front skin	0.953	0.898	1.011	0.112
fascia area	1.001	0.996	1.006	0.710
fascia circumference	1.000	0.994	1.006	0.921
fascia depth	1.007	0.988	1.027	0.478
fascia eccentricity	0.001	0.000	0.381	**0.024** *
fascia width	0.996	0.978	1.013	0.624
spine to back skin	0.967	0.919	1.017	0.195
body area	0.999	0.995	1.003	0.740
body circumference	0.998	0.993	1.004	0.604
vertebral body to fascia	1.017	0.996	1.038	0.116
vertebral body to front skin	1.009	0.989	1.029	0.373
vertebral body height	0.911	0.783	1.061	0.230
Fat				
visceral fat area	1.000	0.993	1.007	0.973
subcutaneous fat area	0.995	0.986	1.004	0.283
subcutaneous fat density (Hu)	1.026	0.979	1.076	0.277
Muscle				

Variable	Hazard Ratio	95% confidence interval		P
very low density mean area	1.118	1.020	1.225	**0.017** *
low density mean area	1.037	0.984	1.092	0.176
normal density mean area	0.976	0.957	0.995	**0.015** *
high density mean area	0.897	0.640	1.255	0.525
dorsal muscle group erector spinae muscle area	0.964	0.920	1.012	0.137
dorsal muscle group erector spinae muscle mean intensity (Hu)	0.950	0.908	0.993	**0.025** *
skeletal muscle area	0.986	0.968	1.004	0.120
skeletal muscle mean intensity (Hu)	0.945	0.898	0.994	**0.029** *
Spine/Bone				
bone mineral density in trabecular bone (Hu)	0.990	0.981	0.999	**0.029** *

* $P < 0.05$

Hu: Hounsfield unit